Application of the MOCABA algorithm and the FSTC tool for source term predictions during severe accident scenarios

A. Stakhanova [a,*], F. Gabrielli [a], V.H. Sanchez-Espinoza [a], A. Hoefer [b], E.M. Pauli [c]

[a] *Karlsruhe Institute of Technology, KIT, Hermann-von-Helmholtz-Platz 1, Eggenstein-Leopoldshafen, Germany*
[b] *Framatome GmbH, Seligenstädter Strasse 100, 63791 Karlstein am Main, Germany*
[c] *Framatome GmbH, Paul Gossen Strasse 100, 91052 Erlangen, Germany*

A R T I C L E I N F O

Keywords:
ASTEC
Fast Source Term Calculation tool
QUENCH-08
KONVOI-1300
Source term prediction

A B S T R A C T

This paper describes the capabilities of the Fast Source Term Calculation (FSTC) tool developed by the Karlsruhe Institute of Technology (KIT) to perform time series predictions of the radiological source term (ST) during severe accident (SA) scenarios. The prediction algorithm implemented in FSTC is based on the MOCABA data assimilation framework, developed by Framatome, and requires a training database and actual measurements. The training database is assessed by employing coupling FSTC to the European reference Accident Source Term Evaluation Code (ASTEC), developed by IRSN. The prediction capabilities of FSTC is applied to evaluate: 1) the mass of released hydrogen during the QUENCH-08 experiment; 2) the xenon release to the environment during a Medium Break Loss of Coolant Accident (MBLOCA) SA scenario in a generic KONVOI nuclear power plant (NPP). The prediction results show a very promising employment of FSTC and the MOCABA algorithm in view of supporting the emergency response team during SA scenarios.

1. Introduction

Real-time information about the progression of a severe accident (SA) at a nuclear power plant (NPP) and of the related radiological source term (ST) is fundamental to initiate a prompt response by the emergency response team and to make proper decisions to manage the event.

SA codes have been developed for some decades to evaluate the progression of SA scenarios at a NPP, from the initiation of the accident up to the release of fission products (FPs) into the environment. Such integral codes, e.g. ASTEC (Chailan et al., 2019; Allelein et al., 2003), MELCOR (Humphries et al., 2015), and MAAP (Luxat et al., 2016), are nowadays employed to calculate Figures-of-Merit (FoMs) related to the in-vessel and ex-vessel accident progression. Furthermore, concerning the ST in particular, efforts have been made to quantify the impact of the uncertainties of the physical models embedded in such codes on the ST-related FoMs. Examples are the SOARCA project (NRC, 2012) and the currently running EC MUSA project (Herranz et al., 2021), within which the Karlsruhe Institute of Technology (KIT) and Framatome jointly participate.

Since the SA code simulations are very time-consuming, such codes cannot be used by the emergency response team of a NPP during a SA to have real-time information on the accident progression. Hence, there is a need for dedicated software that provides relevant information about the course of the accident in real time to the emergency response team. A widely used approach for fast ST prediction is the application of Bayesian Belief Networks (BBNs). It is used in tools like RASTEP (Knochenhauer et al., 2012) and allows for choosing very quickly from a collection of pre-calculated ST values, taking into account answers provided by the personnel about the plant status. The drawback of this approach is that the ST prediction cannot be adjusted to the actual accident progression, which can be expected to be different from any of the pre-calculated variants, due to the high uncertainties and complexity of the process.

In order to overcome such limitations, the WAME project was launched by KIT and Framatome in 2019, with the support by the German Federal Ministry for Economic Affairs and Climate Action – BMWi. The goal of the project is the assessment of a methodology and the development of a tool for fast predictions of the ST during SA scenarios at NPPs. The purpose of this tool is to assist the emergency response team of the NPP in decision-making during the course of an accident.

To obtain realistic ST predictions, the estimation of the ST should be performed in real time and be based not only on pre-calculated ST

* Corresponding author.
E-mail address: anastasia.stakhanova@kit.edu (A. Stakhanova).

values, but also on plant data measured during the SA. For this purpose, the MOCABA data assimilation methodology (Pauli et al., 2022; Hoefer et al., 2015; Castro et al., 2016) is employed, which has been developed by Framatome. An algorithm based the MOCABA approach has been implemented in the Fast Source Term Code (FSTC) (Stakhanova et al., 2022) developed by KIT in the framework of the WAME project. FSTC is used to generate a training database for the prediction model, which consists of results of multiple SA simulations for random-sampled input parameters. The trained prediction model then has the capability to map very fast (practically in real-time) measured data from plant detectors onto predictions of accident variables, such as the ST. The procedure of preparing the training database involves random-sampling of uncertain input parameters, running multiple SA simulations for the sampled input parameters, and uncertainty and sensitivity (U&S) analysis of the simulation results. The latter includes the calculation of correlation coefficients between to-be-measured variables (such as dose rates) and the to-be-predicted ST. This information is used to select for the prediction model an appropriate set of to-be-measured variables that have the potential to provide relevant information with respect to the ST prediction. The functionalities to perform all of the above steps are implemented in the FSTC tool.

Currently, the FSTC tool is coupled with the ASTEC SA code. All simulations presented here have been performed with ASTEC (version 2.2b). ASTEC is developed by the Institute de Radioprotection et de Sûreté Nucléaire (IRSN) and allows to simulate the full range of the in-vessel and ex-vessel phenomena during SA progression. For the ASTEC simulations performed in the context of the current work, all ASTEC modules have been activated – from modeling the release from fuel pellets to aerosol chemistry in the containment.

In the present paper, the time series prediction algorithm described in (Pauli et al., 2022) is applied to two different tasks:

1. The prediction of the hydrogen release for the QUENCH-08 experiment (Stuckert et al., 2005);
2. The prediction of the xenon (Xe) release into the environment in case of an MBLOCA scenario at a KONVOI NPP.

The structure of the paper is the following:

- Section 2 – Brief description of MOCABA algorithm;
- Section 3 – Brief description of FSTC tool structure;
- Section 4 – Prediction algorithm application to the results of QUENCH-08 experiment simulations;
- Section 5 – Prediction algorithm application to the results of MBLOCA SA scenario simulations;
- Section 6 – Conclusions.

2. Mocaba algorithm description

The MOCABA prediction algorithm for time series applications (Pauli et al., 2022) is based on the mathematical framework presented in (Hoefer et al., 2015; Castro et al., 2016). Its purpose is to translate Monte Carlo (MC) simulation data for a set of correlated time-dependent variables and corresponding time-dependent measurements into future predictions of a set of to-be-predicted variables. Details can be found in (Pauli et al., 2022).

The application of the MOCABA time series prediction algorithm involves two main parts – the *'prior'* and the *'posterior'* part. For the *prior* part, the results of *N* Monte Carlo simulations for the to-be-predicted variables and the to-be-measured variables are used as training data. In the *prior* part, the prior distribution model parameters of the MOCABA model are calculated, i.e. the mean values of the considered variables, covariances between different variables for each time step, and covariances between different time steps for each variable.

In the *posterior* part, measurement information for the to-be-measured variables is taken into account by applying Bayesian updating to the prior model parameters. The updating is performed in two steps. In the first updating step, the posterior model parameters are calculated for all observed time steps until the current point in time. In the second updating step, predictions are performed for the time steps lying in the future. As described in detail in (Pauli et al., 2022), the second updating step is defined by an iterative procedure involving several substeps. Fig. 1 provides an illustration of that procedure. In the initial substep, the posterior variable values Y^*, corresponding to the current time step and to a certain number Δ_t of previous time steps (calculated in the first updating step), are identified with a set of 'measurements' to calculate the posterior variable values Y_+^* for a certain number Δ_t^+ of future time steps. This updating step is, in particular, determined by the prior cross-covariances Cov_+ between Y^* and Y_+^* (see Fig. 2). In the next substep, the updating procedure of the initial substep is repeated, now identifying the latest Y_+^* value with the new 'current' time step. Repeating this updating procedure for the following substeps, finally leads to the posterior predictions of the variable values at all considered future time steps.

In the next section, the description of the FSTC tool is presented, where the MOCABA algorithm and functionality for performing U&S analysis are implemented.

3. FSTC tool description

The FSTC tool has been developed by KIT in the Institute for Neutron Physics and Reactor Technology (INR) in the framework of the WAME project. A more detailed description can be found in (Stakhanova et al., 2022). In the following, only a brief summary is presented. The FSTC tool can be divided into two main parts (see Fig. 3). The first part has the task to perform U&S analysis and to generate the training database for the prediction algorithm. The second part contains an implementation of the prediction algorithm described above.

To perform the U&S analysis, the user specifies a list of uncertain input parameters to be sampled, as well as their probability density functions (PDFs) and PDFs' parameters. The choice of the PDFs are based on the available information from the literature and engineering judgement. Currently available PDFs in the tool are uniform, normal, truncated normal, triangular, and beta. Currently available sampling methods are Simple Random Sampling (SRS) and Latin Hypercube Sampling (LHS) (McKay et al., 1979). The user also can specify correlations between input parameters; in that case, the Iman-Conover (Iman and Conover, 1982) method is employed to rearrange the sampled values according to the provided correlation matrix.

After that, multiple ASTEC simulations are run in parallel. Each individual simulation run has its own set of values for the uncertain input parameters. When all simulations are finished, FSTC checks whether they finished correctly and excludes the failed ones.

The user provides the list of the parameters of interest, which shall be analyzed in the U&S part of the code, and FSTC collects the data for these parameters from the ASTEC output files for all correctly finished simulations. The user also can specify for which time interval the U&S analysis shall be performed. The code will take the data only for that interval and provide it to the U&S part of the code.

At the final step in the U&S part of the FSTC tool, simple statistics and different correlation coefficients (Pearson, Spearman, etc.) are calculated. One of the outputs from the U&S analysis part – the results of multiple code runs – is also used as input for the prediction part of FSTC. That data is used as input for the *prior* part of the MOCABA algorithm. If real measurements are not available, the predictive power of the MOCABA algorithm can be tested by treating the results of individual ASTEC simulations as "measurements" and using them as input for the *posterior* part of the MOCABA algorithm.

In the next section, the QUENCH-08 experiment and its corresponding ASTEC model are briefly described.

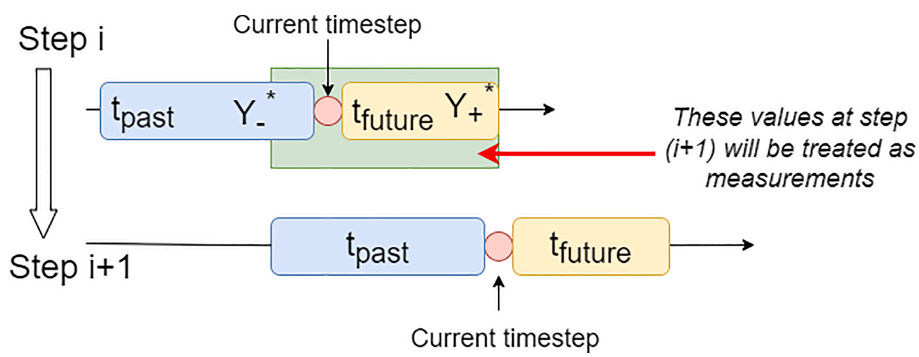

Fig. 1. Posterior part of MOCABA algorithm: Illustration of updating procedure for future predictions.

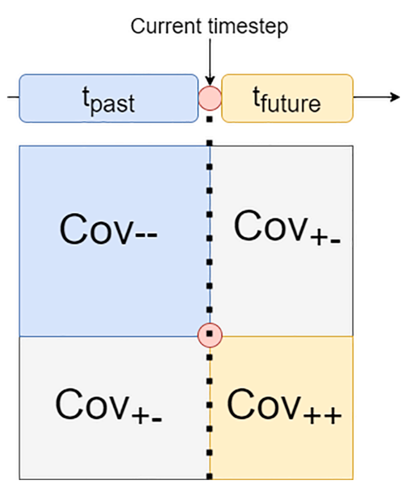

Fig. 2. Covariance matrix of variable values at past and future time steps.

4. Prediction algorithm application to the results of quench-08 experiment simulations

4.1. Description of quench-08 experiment and its corresponding ASTEC model

The QUENCH-08 experiment (Stuckert et al., 2005) was performed in 2003 at the Forschungszentrum Karlsruhe (FZK) in the frame of the QUENCH program. The aim of the experiment was to investigate the hydrogen source term and material interactions during LOCA and the early phase of severe accidents including reflood in a fuel rod bundle.

The test bundle consists of 21 fuel rod simulators. 20 of them are heated by tungsten elements mounted inside the simulators and the central one remains unheated. These 21 simulators plus 4 corner rods are located inside a Zircaloy shroud, which is surrounded by insulation enveloped by cooling jacket. The central rod and eight rods around it were combined into one structure in the ASTEC model – *'Channel_1'*, the rest of the rod simulators and four corner rods form another structure – *'Channel_2'*, shroud, insulation and cooling jacket are also simulated, see Fig. 4(left-hand side).

Thermocouples are attached to each fuel rod simulator at different elevations and angles, the shroud and the cooling jacket, and the axial nodalization in the ASTEC model allows to calculated the temperature values of different model structures at different elevations, see Fig. 4 (right-hand side).

The experiment consisted of 5 main phases (Stakhanova et al., 2022; Stuckert et al., 2005):

1. Heat-up to ~873 K, $t = 0$–134 s;
2. Heat-up to ~1700 K with a rate of ~0.3–0.6 K/s, $t = 134$–2277 s;
3. Pre-oxidation phase: maintaining the constant temperature when superheated steam flowed through the test bundle, $t = 2277$–3240 s;
4. Transient phase: the temperature increasing up to 2200 K, $t =$ 3240–3814 s;
5. Cooling down with saturated steam injected from the bottom of the test section, $t =$ 3775.5–4647 s (end of the test). During that time period electric power reduction up to 3.9 kW is performed (from $t =$ 3830 s);

In the next section, the results of the ASTEC simulations for the presented QUENCH-08 model are briefly described.

4.2. Simple statistics of simulation results

In the current section, only simple statistics results of QUENCH-08 simulations are shown. Details of the U&S analysis were presented in

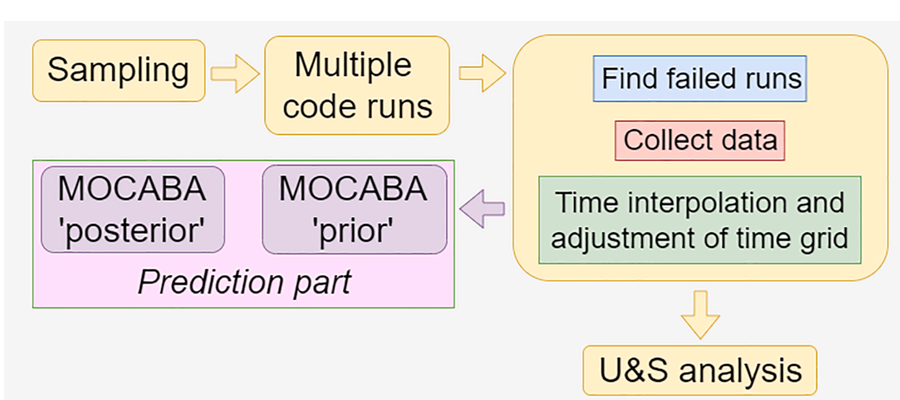

Fig. 3. FSTC tool scheme.

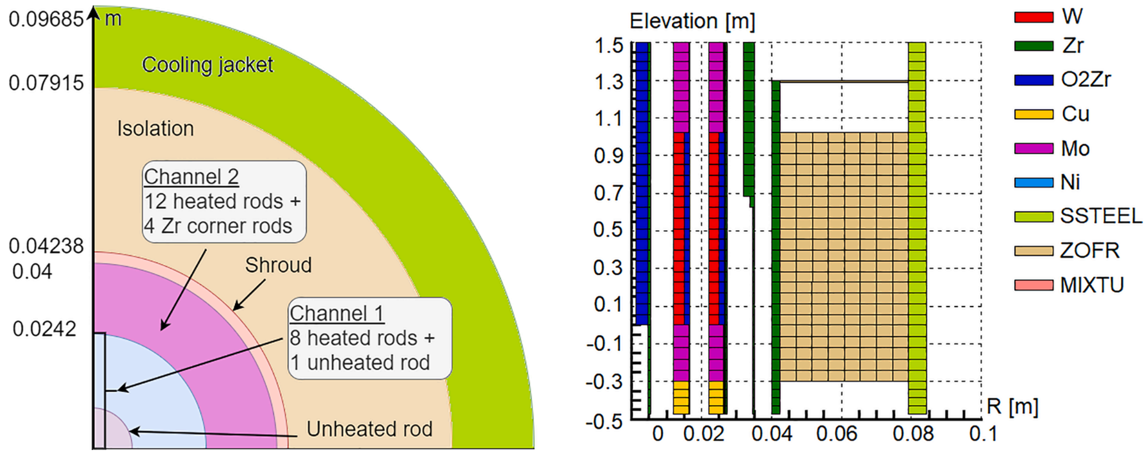

Fig. 4. ASTEC model of QUENCH-08 experiment.

(Stakhanova et al., 2022). Here, for the purpose of demonstrating the application of the MOCABA algorithm only simple statistics of chosen *'prediction'* and *'observable'* parameters are needed.

To prepare the training database for the *prior* part of the prediction algorithm, 400 ASTEC simulations were run. 24 uncertain input parameters were used for sampling – 5 of them have a normal distribution and the rest have a uniform distribution. These parameters are related to geometry, initial and boundary conditions and some ASTEC models, like corium relocation model or model of melt oxidation by steam, for example. All details about the choice of these uncertain parameters, their PDFs, PDFs' parameters and links to the literature are also provided in (Stakhanova et al., 2022).

For the purpose of the MOCABA test considered here, the standard deviations of the two most influential parameters – steam flow rate (*stFlow*) and argon flow rate (*arFlow*) – were set to 20 %, while in (Stakhanova et al., 2022) they were set to 5 %. The reason for choosing increased standard deviations is to cover a broader range of possible variants of process progression.

Despite the fact that the experimental results of the QUENCH-08 experiment can be used for testing the prediction algorithm, here only simulation results are used. Using simulated data instead of experimental allows one to test the algorithm in a more systematic way. For that purpose, a set of 50 simulations was prepared with 5 % standard deviation for the *stFlow* and *arFlow* parameters. This guarantees that the results of these 50 simulations will lie inside the uncertainty range of the *prior* input data. In addition, each of these 50 simulations can be used as an individual *'experiment'*.

For that test, three parameters were chosen as *'observables':* temperature of the *'Channel_1'* structure at *950 mm* elevation (*T2_950*), temperature of the *'Channel_2'* structure at *850 mm* elevation (*T3_850*), and shroud temperature at *950 mm* elevation (*TS_950*). Using that data, the generated hydrogen mass (*H2mass*) is to be predicted.

Simple statistics and individual curves for all samples for the amount of produced hydrogen during the course of the process for 400 and 50 samples sets are shown in Figs. 5 and 6, respectively. One can see that the range in which the hydrogen mass varies is especially large for the case with 400 samples, for which the uncertainty for the input parameters was increased. Also, one can notice that the start of massive hydrogen generation can significantly vary – from ~1800 s to ~3800 s.

In the next section, results of the MOCABA application to these sets of data are given.

4.3. Results of hydrogen mass prediction

Two sets of ASTEC QUENCH-08 simulations described in the previous section were used to test the MOCABA time series algorithm. The larger set with results from 400 simulations was used as training database for the *prior* part. The small set of 50 simulations was used as a collection of simulated *'experiments'*. The quantity to be predicted is the hydrogen mass (*H2mass*) based on measurements of three temperature values: temperature of inner circle of fuel rods simulators (in ASTEC model marked as *'Channel_1'* at Fig. 4) at 950 mm elevation – *T2_950*; temperature of outer circle of fuel rods simulators (*'Channel_2'* at Fig. 4) at 850 mm elevation – *T3_850*; and shroud temperature at 950 mm elevation – *TS_950*.

The MOCABA test was performed in the following way:

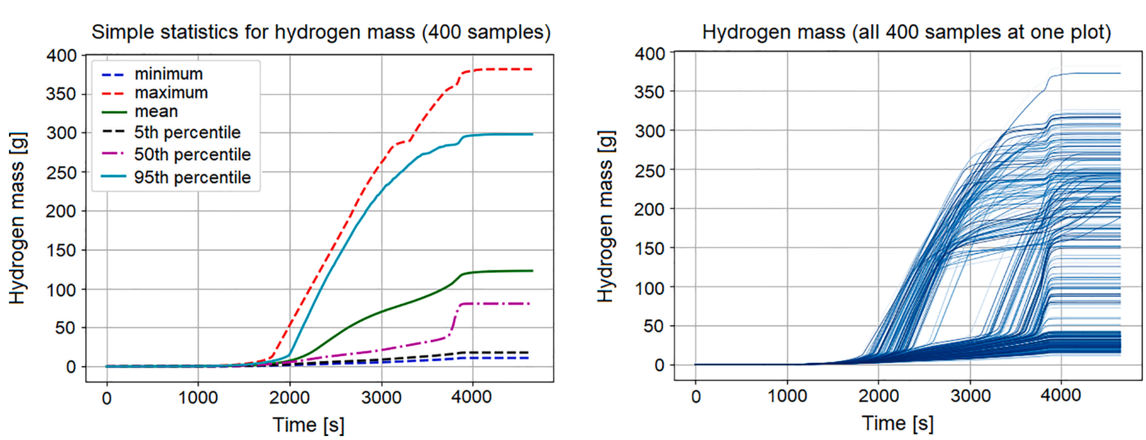

Fig. 5. Simple statistics (left) and hydrogen mass curves for all samples (right) – 400 samples, 20% uncertainty for *stFlow* and *arFlow*.

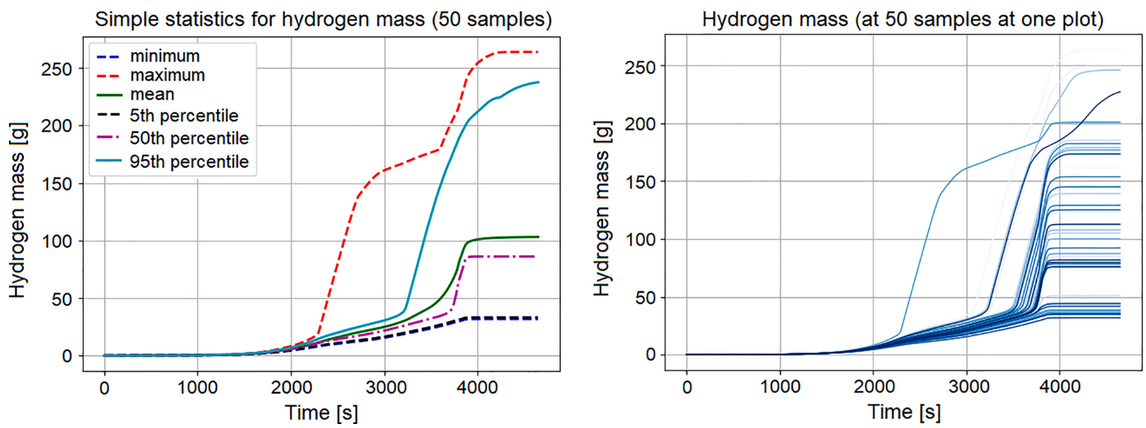

Fig. 6. Simple statistics (left) and hydrogen mass curves for all samples (right) – 50 samples, 5% uncertainty for *stFlow* and *arFlow*.

- Run *prior* part of the algorithm using the set of 400 ASTEC simulation results, which will calculate the prior mean values of the *observable* and the *prediction* parameters, as well as correlations between them at each time step and correlations between the values of each of these parameters for different time steps (in the current implementation of the MOCABA algorithm in the FSTC tool, correlations are translated into covariances in the *posterior* part);
- Consider each example from the set of 50 simulations as an individual *experiment*:
  - Input for calculating the posterior hydrogen mass are the prior results and the *T2_950, T3_850,* and *TS_950* temperature values, which are considered as *measurements*;
  - The *posterior* part calculates the predictions of hydrogen mass values (*H2mass*);
  - Compare predicted *H2mass* values to *H2mass* values of the corresponding simulations provided by ASTEC for that Monte Carlo sample.

In Fig. 7, Pearson correlations between *prediction* and *observable* parameters are presented. High correlation values between these two groups of parameters are important for good predictions. From Fig. 7 it is clear that data prepared for this test meets this requirement. The correlations for each *prediction* - *observable* pair are high over the entire time period, except for the very beginning of the process.

Another requirement for applying the MOCABA algorithm is that the measured values should lie inside the range covered by the *'prior'* data. In our case, the temperature values should lie between the maximum and minimum temperature curves from the set of 400 simulations prepared for the *prior* part. For demonstration purposes, data for two samples (№7 and №11) from the set of 50 samples are here chosen as

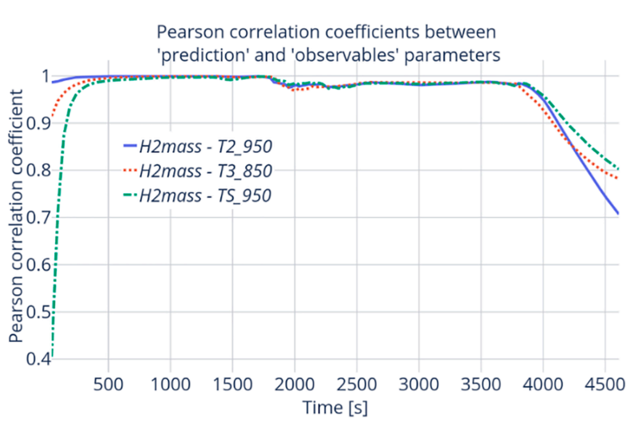

Fig. 7. Pearson correlation coefficients between *prediction* and *observable* variables (MOCABA test on QUENCH-08 simulations).

measurements. In Fig. 8**,** it is shown that the values of *prediction* and *observable* parameters from these two samples are lying inside the range covered by the *prior* data. The maximum curves reflect the high uncertainty of 20 % for steam and argon flow rate in the ASTEC calculations.

On the left-hand side of Figs. 9 and 10, the prediction results for the two selected samples are presented. Measured data is added time step by time step to see how the prediction changes over time. In the figures below, only four predictions are presented, when measurements up to 165, 2442, 3415 and 4485 s were taken into account. *'Experimental'* data is available from 165 s. Hence, only one measured value is available to be used for the prediction. Therefore, the prediction is located close to the prior curve; for sample № 11 the prediction and prior curves are practically identical. Adding more and more measured data, the prediction curve is getting closer and closer to the *experimental* curve. Prediction errors are shown on the right-hand side of Figs. 9 and 10. The error, in general, is decreasing when adding more measured data, except for the very end of the process, where the error increases sharply, probably due to a decrease of the Pearson correlation coefficient between *prediction* and *observable* parameters (see Fig. 7).

In general, good prediction results can be obtained for the QUENCH-08 case.

5. Prediction algorithm application to the results of mbloca sa scenario simulations

5.1. Description of the KONVOI NPP, its ASTEC model, and MBLOCA scenario

Another test for the MOCABA prediction algorithm was made for KONVOI NPP simulations with ASTEC. The original input deck developed by KIT in the frame of the CESAM project (Nowack et al., 2018; García-Toraño, 2017) has been further extended and improved (Gabrielli et al., 2021). All the ASTEC calculation modules are activated in order to simulate the in-vessel and ex-vessel accident progression from the initiation up to the radiological release to the environment. Attention has been paid in a quite detailed modeling of the transport of the fission products from the primary to the containment. With respect to that, a library of realistic fuel inventories for an equilibrium cycle with 328 effective full power days have been computed for performing the ASTEC analyses. For such evaluations, the core is loaded with 193 Fuel Assemblies (48 U FAs, 6 batches; 81 U-Gd FAs, 6 batches; 64 MOX FAs, 4 batches). For the depletion calculations, the ORIGEN-ARP tool has been used, employing the ORIGEN reactor libraries for an 18x18 FA design embedded in SCALE 6.2.3 (Wieselquist et al., 2020).

The core and containment nodalization of the ASTEC model of a generic KONVOI NPP are shown in Fig. 11. The containment is divided into two almost symmetrical halves, with the exceptions of some spaces such as sump, cavity, reactor room and dome. In the model, smaller

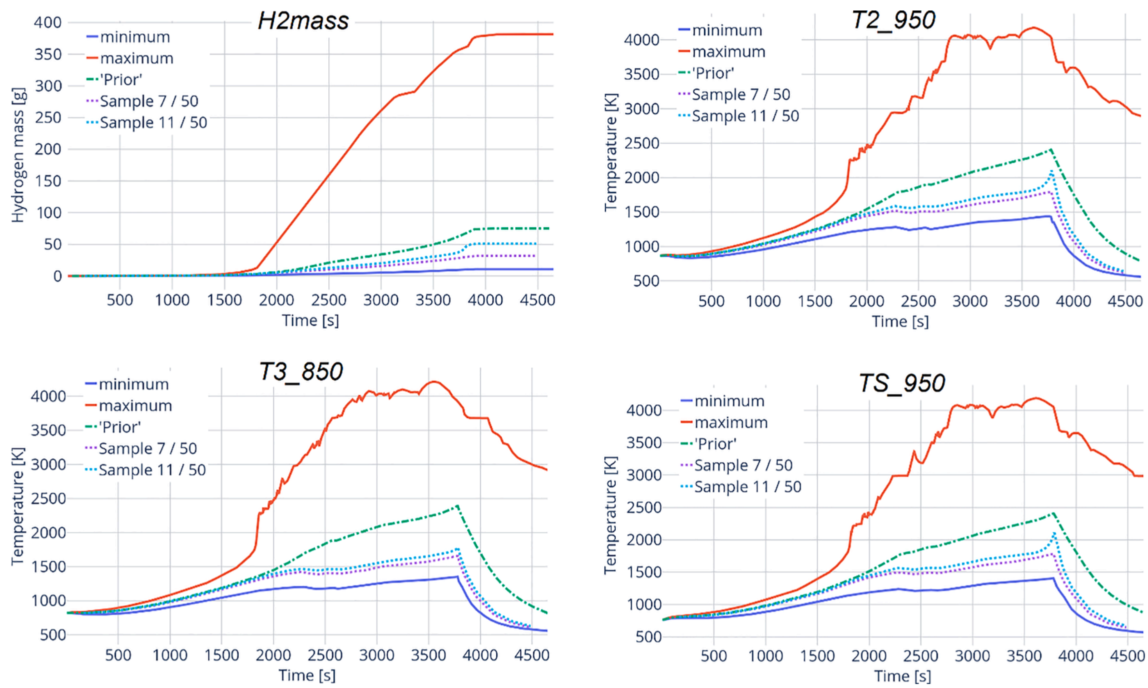

Fig. 8. Prior values for hydrogen mass, temperatures and data for two samples from validation set (MOCABA test on QUENCH-08 simulations).

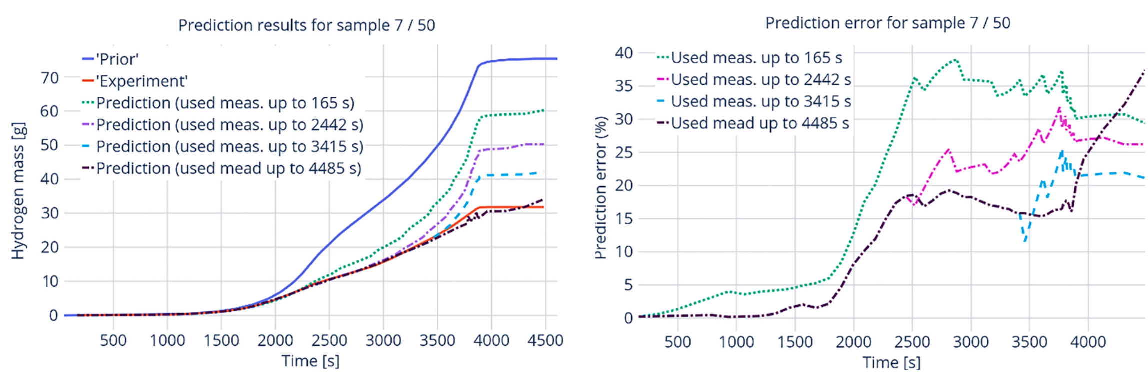

Fig. 9. Prediction results and prediction error for sample №7.

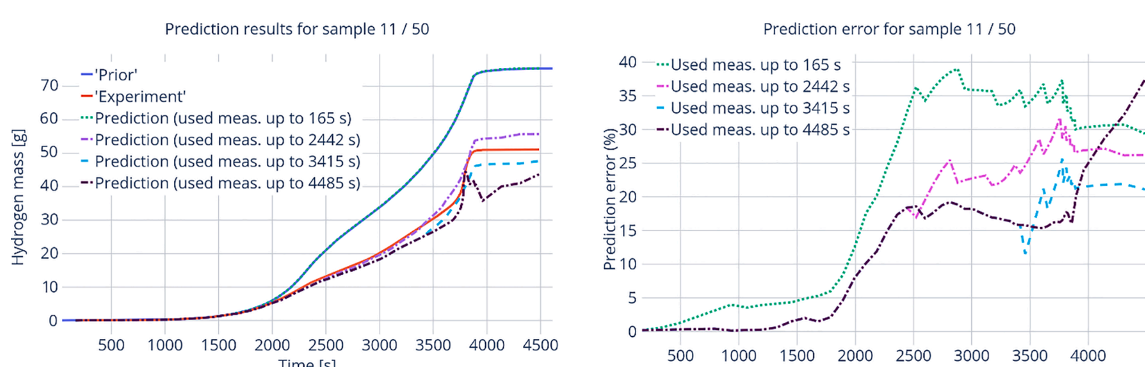

Fig. 10. Prediction results and prediction error for sample №11.

spaces are combined with the adjacent rooms. The plant rooms (green, red, grey, and light blue boxes in Fig. 11) and the operating rooms (white boxes in Fig. 11) are modelled by means of eleven and nine volumes, respectively. Finally, three volumes are employed to model the annulus region (light yellow boxes in Fig. 11). The containment and the annulus, as well as the annulus and the environment, are connected by means of two fans. The flow rates through such fans depend in the model on the relative pressure differences in such zones based on plant data.

The MBLOCA scenario (with 0.044 m^2 break in the cold leg) is considered in this work. Simulations were stopped 6000 s after lower

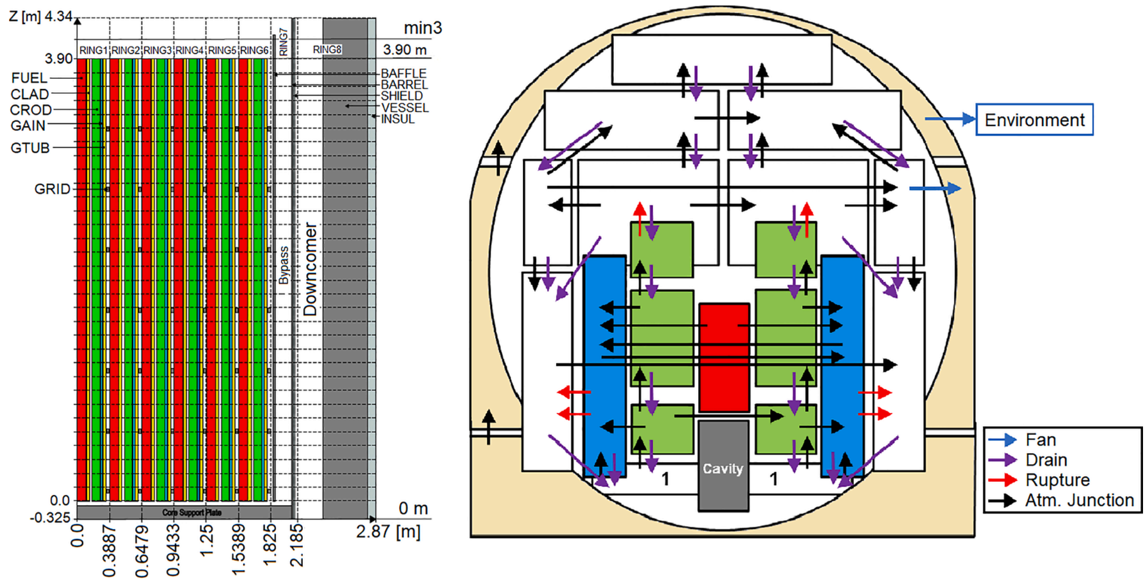

Fig. 11. Core and containment nodalizations of KONVOI ASTEC model. From (Wieselquist et al., 2020).

head vessel failure.

The progression of the events of the MBLOCA scenario have been modeled in the ASTEC input deck as follows:

1. Break of the cold leg at t = 0 s;
2. Reactor scram, if the primary pressure is lower than $1.32{\cdot}10^7$ Pa or containment overpressure is larger than $3{\cdot}10^3$ Pa;
3. No admission to turbine and closure of the main feed water pumps into the steam generator;
4. Emergency Core Cooling System (ECCS) is activated if two of the following three conditions are fulfilled: containment overpressure larger than $3{\cdot}10^3$ Pa; pressure of the Reactor Coolant System (RCS) lower than $1.10{\cdot}10^7$ Pa; pressurizer liquid level lower than 2.30 m;
5. Main Coolant Pumps are coasted down and the pressure regulation in the pressurizer is switched off;
6. Activation of the Emergency Feed Water System (EFWS) when the liquid level of one SG falls below 4.50 m;
7. High and low pressure injection systems (HPIS and LPIS) activated when the temperature of the gas in the primary exceeds 923 K, and continue to work until tanks are empty. In this condition, the severe accident occurs;
8. Activation of the Extra Borating System when the pressurizer water level is lower than 2.30 m;

5.2. Simple statistics of simulation results

To test the MOCABA prediction algorithm for the KONVOI MBLOCA simulations, two separate sets of data were prepared, one with 300 and one with 100 samples. Some of the ASTEC simulations failed for different reasons. Some simulations, which had a very fast accident progression, were excluded to provide a broader time range for U&S analysis. The resulting number of samples used for calculating *'priors'* and *'posteriors'* were 255 and 89 samples, respectively.

Simple statistics are only briefly described here to demonstrate how the prediction parameters are changing in time. Unlike for the QUENCH-08 simulations, the uncertainty ranges of input parameters were chosen the same for the 255 and the 89 sample set. Nevertheless, data from the smaller set is covered by the data of the larger set, which is used for *prior* part.

16 uncertain input parameters were used in both cases: 6 with normal distribution, 5 with triangular distribution, 4 with uniform distribution, and one with beta distribution. These parameters are related to different ASTEC models – release of FPs from fuel pellets, integrity criteria, aerosol behavior. In addition, there are parameters governing the leakage flow rate from containment to annulus and burnup. The release into the environment is mostly defined by two uncertain input parameters, one governing the leakage rate from the annulus to the environment and the second one governing the burnup. For the release into the containment, the most important parameter is the one related to the burnup. For these two parameters, the Spearman correlation to the release to the environment amounts to up to 0.9. Other parameters have smaller Spearman coefficient values. For example, the Spearman correlation between the release of low-volatile fission products, like Ba and Mo, into the vessel and the primary circuit and parameters from the ELSA ASTEC model (models the release from the fuel pellets) is around 0.4 at the beginning of the SA. Parameters from the SOPHAEROS ASTEC module (models aerosols behavior in containment and primary circuit) affects Cs and I aerosols release into the containment at later stages of the SA (Stakhanova et al., 2022). A detailed description of the assessment of the PDFs of the uncertain parameters and of the results of the U&S analysis is presented in (Stakhanova et al., 2022). Note that in the presented simulations, the containment integrity was not compromised. Table 1 shows the time range for the occurrence of some characteristic events. Changing uncertain parameters values could significantly affect SA progression, for example, difference between the earliest time of the lower head vessel failure and the latest one is almost 15 times.

For the MOCABA test for the KONVOI simulations, the amount of Xe as a fraction of the initial inventory released to the environment (*XetEFr*) has been chosen as *observable*. Simple statistics and curves for all samples for *XetEFr* are presented on the left-hand side and right-hand side of Figs. 12 and 13, respectively. One can see that there is no big difference between the shapes of the curves, like for the hydrogen mass curves in Figs. 5 and 6.

Table 1
Time range of main events occurring during SA progression. (From results of 300 simulations of MBLOCA scenario).

Event	*Minimum time (s)*	*Maximum time (s)*
Start of FPs release from the fuel pellets	424.4	764.4
First corium slump into the lower plenum	724.4	11784.4
Lower head vessel failure	2240.9	33206.9
End of the corium slump from the lower head to the cavity	2243.2	33225.6

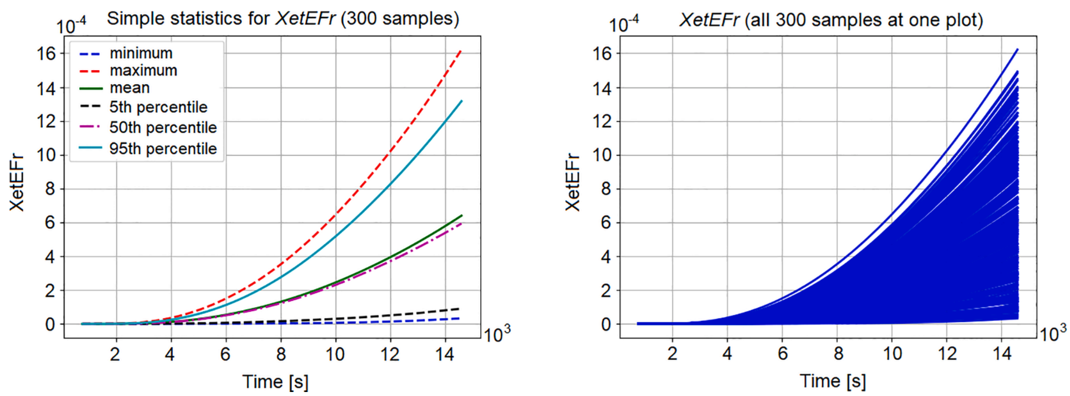

Fig. 12. Simple statistics (left) and Xe released to the environment for all samples (right) – 255 samples.

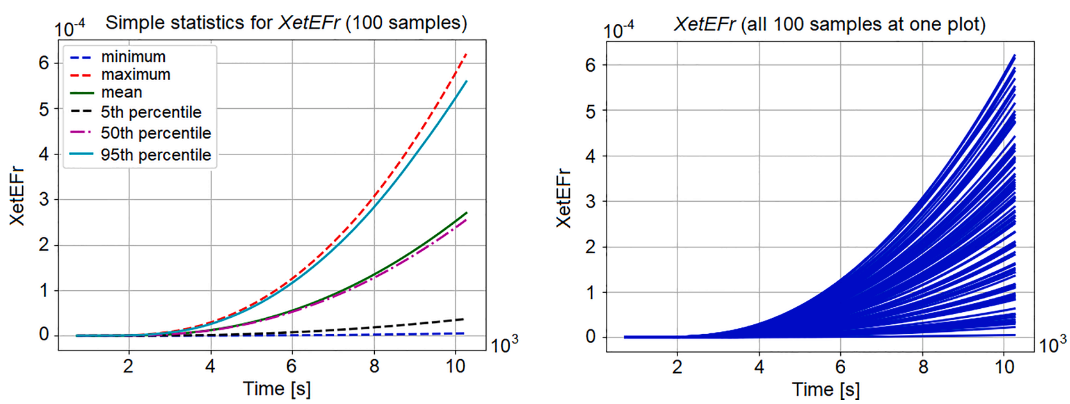

Fig. 13. Simple statistics (left) and Xe released to the environment for all samples (right) – 89 samples.

In the next section, the results of the MOCABA prediction for the KONVOI MBLOCA simulations are presented.

5.3. Results of xenon release prediction

The test of the MOCABA prediction algorithm was performed as described in Section 6. A set of simulations (with smaller amount of samples) was used as a collection of individual *'experiments'*, and MOCABA was applied to these *'experiments'* one by one. As stated before, the correlations between *'prediction'* and *'observable'* variables should be high in order to obtain good predictions for given values of the *'observable'* variables. Two possible candidates for observable parameters were suggested – total dose rate in annulus (*TotalDoseAnnulus*) and total dose rate in containment (*TotalDoseCont*). Pearson correlation coefficients between the *'observable'* and the chosen *'prediction'* parameters are shown at Fig. 14. As one can see, the correlation between *TotalDoseCont* and *XetEFr* is fairly low, especially after 8000 s. Therefore, *TotalDoseCont* was excluded from the prediction model. The correlation between *TotalDoseAnnulus* and *XetEFr*, on the contrary, is very high over the entire time period. *TotalDoseAnnulus* is, therefore, chosen as a suitable *'observable'* parameter for the MOCABA prediction model.

Two samples were chosen for demonstration purpose – samples №2 and №59. It is shown in Fig. 15 that *XetEFr* and *TotalDoseAnnulus* values for these two samples are lying inside the uncertainty range of the *prior* data.

Prediction results for samples №2 and №59 are presented on the left-hand side of Figs. 16 and 17, and prediction errors are shown on the right-hand side of these figures. As for the QUENCH-08 example, four prediction curves are presented for each considered sample, which correspond to four different points in time at which the predictions are performed. The more measured data are used the better the prediction

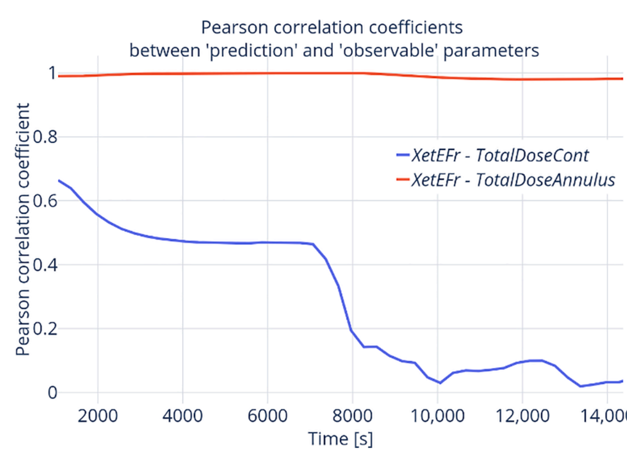

Fig. 14. Pearson correlation coefficients between 'prediction' and 'observable' variables (test MOCABA on KONVOI MBLOCA simulations).

becomes. The very high prediction error (in %) at the beginning of the process is due to the very small values of the released amount of Xe at that time. The prediction error decreases very fast with time and is around 10 % already when measured data up to 5614 s is used.

6. Conclusions

A time series prediction algorithm based on the MOCABA data assimilation framework was tested on two different application cases:

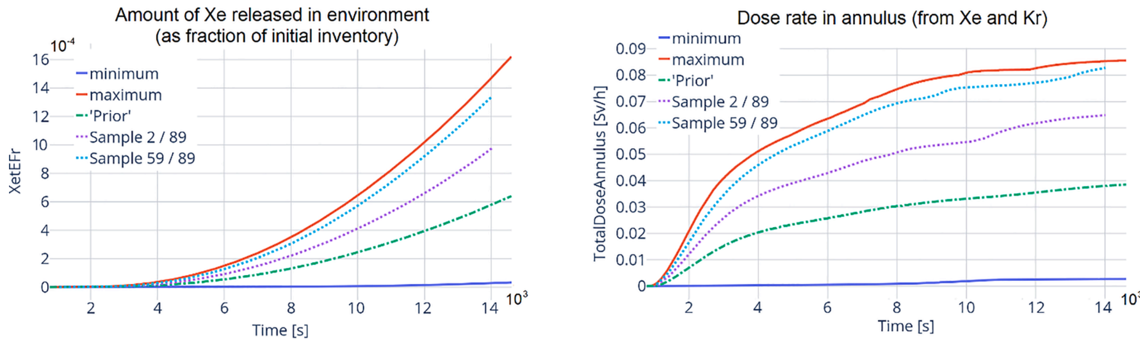

Fig. 15. *Prior* values for amount of Xe released into the environment, total dose rate in annulus and data for two samples from validation set.

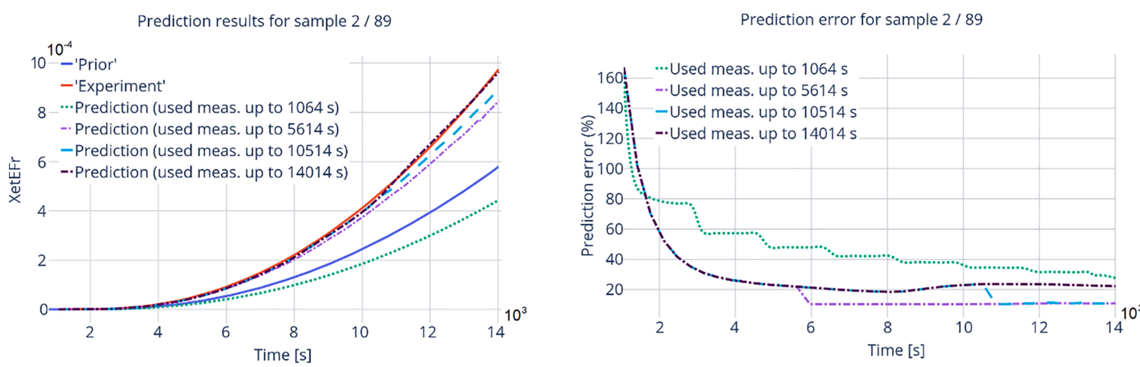

Fig. 16. Prediction results and prediction error for sample №2.

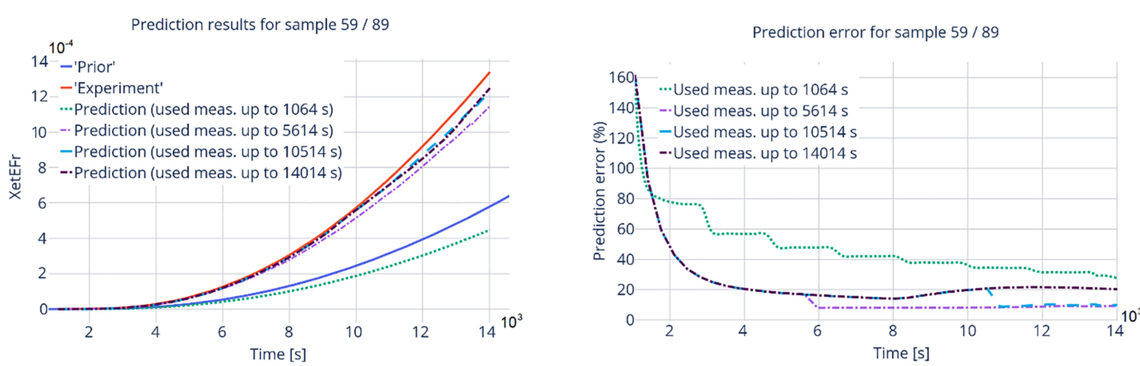

Fig. 17. Prediction results and prediction error for sample №59.

- Prediction of the amount of generated hydrogen for the QUENCH-08 experiment using as measurements the temperatures at different elevations;
- Prediction of the amount of Xe released to the environment for an MBLOCA SA scenario at a KONVOI NPP using as measurements the values of the total dose rate in the annulus.

The FSTC tool (developed by KIT) was applied to the ASTEC SA code to perform Monte Carlo uncertainty propagation for the QUENCH-08 experiment and for an MBLOCA SA scenario at a KONVOI NPP. The simulation results were then used by FSTC to perform U&S analysis and to train the MOCABA prediction model. To test the performance of the trained prediction model, the prediction algorithm (also implemented in FSTC) was applied to selected ASTEC simulations, which were chosen as application cases. The simulated application case measurements were here applied to the trained prediction model, and the obtained predictions of the to-be-predicted variables (generated hydrogen or released Xe) were compared to the actual values of the selected application cases.

From the results of the performed test cases it can be concluded that the MOCABA time series prediction algorithm can be very useful to perform real-time predictions of accidents at nuclear power plants based on measured plant data. Implementing MOCABA prediction models for different accident scenarios within specific software packages, such as Framatome's Central Radiological Computer System (CRCS) (Torchiani et al., 2015), may significantly improve the safety level of a NPP by automatically providing the emergency response team with real-time information about the course of an accident.

A necessary precondition for generating a reliable prediction model, however, is that the modeling of the accident (e.g. in terms of an ASTEC model) is sufficiently representative of the NPP to which the prediction model shall be applied. Also the uncertainties represented by the PDFs of the input parameters shall sufficiently cover the actual uncertainties we have to deal with for the NPP under consideration. A further precondition for reliable predictions is that measured plant data are available that are sufficiently high correlated to the to-be-predicted quantities

(Pauli et al., 2022). For example, for the analyzed MBLOCA SA scenario, the annulus dose rate was highly correlated to the Xe release to the environment, which made the annulus dose rate a suitable measurement variable for the prediction model of the Xe release. Finally, there may be cases where the simulated time curves corresponding to different sets of sampled input parameters show significantly different shapes and many crossings, similar to a ball of wool (Pauli et al., 2022). If this is the case, the available measurement information at a given time during the accident provides only limited information about the further course of the accident. In the context of a prediction model this situation reflects a low information content of the training data, which reduces the predictive power of the trained prediction model.

CRediT authorship contribution statement

A. Stakhanova: Conceptualization, Software, Writing – original draft, Visualization. **F. Gabrielli:** Conceptualization, Writing – review & editing, Supervision. **V.H. Sanchez-Espinoza:** Conceptualization, Writing – review & editing, Supervision, Project administration, Funding acquisition. **A. Hoefer:** Formal analysis, Software, Writing – review & editing. **E.M. Pauli:** Formal analysis, Writing – review & editing.

Declaration of Competing Interest

The authors declare that they have no known competing financial interests or personal relationships that could have appeared to influence the work reported in this paper.

Data availability

The authors do not have permission to share data.

Acknowledgements

The project was funded by the German Federal Ministry of Economic Affairs and Energy, funding code FZK 1501582 (WAME project).

References

Allelein, H.J., Neu, K., Van Dorsselaere, J.P., Müller, K., Kostka, P., Barnak, M., Matejovic, P., Bujan, A., Slaby, J., 2003. European validation of the integral code ASTEC (EVITA). Nucl. Eng. Design 221 (1–3), 95–118.

Castro, E., Ahnert, C., Buss, O., Garcia-Herranz, N., Hoefer, A., Porsch, D., 2016. Improving PWR core simulations by Monte Carlo uncertainty analysis and Bayesian inference. Ann. Nucl. Energy 95, 148–156.

Chailan, L., Bosland, L., Carénini, L., Chambarel, J., Cousin, F., Chatelard, P., Drai, P., Kioseyian, G., Phoudiah, S., Topin, V., 2019. Overview of ASTEC integral code status and perspectives. 9th European Review Meeting on Severe Accident Research (ERMSAR2019), March 18–20. Clarion Congress Hotel, Prague, Czech Republic.

Gabrielli, F., Sánchez-Espinoza, V.H., Stakhanova, A., Hoefer, A., Pauli, E., Feldmann, H., 2021. Source term evaluation following MBLOCA and SBLOCA scenarios in a generic KONVOI-1300 NPP by means of the ASTEC Code. Eurosafe 22–23.

García-Toraño, I.G., 2017. Further Development of Severe Accident Management Strategies for a German PWR Konvoi Plant based on the European Severe Accident Code ASTEC. Doctoral dissertation. Karlsruhe Institut für Technologie (KIT).

Herranz L.E. at al., 2021. The EC MUSA Project on Management and Uncertainty of Severe Accidents: Main Pillars and Status, Energies, 14.

Hoefer, A., Buss, O., Hennebach, M., Schmid, M., Porsch, D., 2015. MOCABA: A general Monte Carlo-Bayes procedure for improved predictions of integral functions of nuclear data. Ann. Nucl. Energy 77, 514–521.

Humphries L.L., Figueroa V.G., Young M.F., Louie D., Reynolds J.T., 2015. *MELCOR Computer Code Manuals* (No. SAND-2015-6692R), Sandia National Lab. (SNL-NM), Albuquerque, NM (United States).

Iman, R.L., Conover, W.J., 1982. A distribution-free approach to inducing rank correlation among input variables. Commun. Stat. Simul. Comput. 11 (3), 311–334.

Knochenhauer M., Swaling V.H., Alfheim P., 2012. *Using Bayesian Belief Network (BBN) modelling for Rapid Source Term Prediction. RASTEP Phase 1* (No. NKS–267). Nordisk Kernesikkerhedsforskning.

Luxat, D.L., Kalanich, D.A., Hanophy, J.T., Gauntt, R.O., Wachowiak, R.M., 2016. MAAP-MELCOR crosswalk phase 1 study. Nucl. Technol. 196 (3), 684–697.

McKay, M.D., Beckman, R.J., Conover, W.J., 1979. A comparison of three methods for selecting values of input variables in the analysis of output from a computer code. Technometrics 21 (2), 239–245.

Nowack, H., Chatelard, P., Chailan, L., Hermsmeyer, S.t., Sanchez, V., Herranz, L., 2018. CESAM–Code for European severe accident management, EURATOM project on ASTEC improvement. Ann. Nucl. Energy 116, 128–136.

NRC, U., 2012. State-of-the-Art Reactor Consequence Analyses (SOARCA) report (NUREG-1935).

Pauli, E.-M., Hoefer, A., Gabrielli, F., Stakhanova, A., Sanchez-Espinoza, V.H., 2022. Prediction of the radiological consequences of a severe accident scenario in a generic Konvoi nuclear power plant. 10th European Review Meeting on Severe Accident research (ERMSAR2022), May 16–19. Akademiehotel, Karlsruhe, Germany.

Stakhanova, A., Gabrielli, F., Sanchez-Espinoza, V.H., Pauli, E.-M., Hoefer, A., 2022. Uncertainty and sensitivity analysis of the ASTEC simulation results of a MBLOCA scenario in a generic KONVOI plant using the FSTC tool. 10th European Review Meeting on Severe Accident research (ERMSAR2022), May 16–19. Akademiehotel, Karlsruhe, Germany.

Stakhanova, A., Gabrielli, F., Sanchez-Espinoza, V.H., Hoefer, A., Pauli, E., 2022. Uncertainty and sensitivity analysis of the QUENCH-08 experiment using the FSTC tool. Ann. Nucl. Energy 169, 108968.

Stuckert J., Boldyrev A.V., Miassoedov A., 2005. Experimental and computational results of the QUENCH-08 experiment (reference to QUENCH-07) (No. FZKA–6970). Forschungszentrum Karlsruhe GmbH Technik und Umwelt (Germany). Inst. fuer Materialforschung.

Torchiani S., Buss O., Haussler S., Ludwik O., Hoefer A, AREVA computer codes for radiological consequence analysis. In: International Experts Meeting on Assessment and Prognosis in Response to a Nuclear or Radiological Emergency, IAEA, Vienna, Austria, April 20 – 24 (2015) https://www-pub.iaea.org/iaeameetings/IEM9p/Session2/6Torchiani.pdf.

Wieselquist W.A., Lefebvre R.A., Jessee, M.A., 2020. SCALE Code System, ORNL/TM-2005/39, Version 6.2. 4. *Oak Ridge National Laboratory, Oak Ridge, TN.*